

Deep Network Uncertainty Maps for Indoor Navigation

Jens Lundell*, Francesco Verdoja* and Ville Kyrki

Abstract—Estimating the uncertainty of predictions is a crucial ability for robots in unstructured environments. Most mobile robots for indoor use rely on 2D laser scanners for localization, mapping and navigation. These sensors, however, cannot detect transparent surfaces or measure the full occupancy of complex objects such as tables. Deep Neural Networks have recently been proposed to overcome this limitation by learning to estimate object occupancy. These estimates are nevertheless subject to noise, making the evaluation of their confidence an important issue. In this work we study uncertainty estimation in deep models, proposing a novel solution based on a fully convolutional autoencoder. The proposed architecture is not restricted by the assumption that the uncertainty follows a Gaussian model, as in the case of many popular solutions for deep model uncertainty estimation, *e.g.*, MC Dropout. We present results showing that uncertainty over obstacle distances is actually better modeled with a Laplace distribution. As an example of application where uncertainty evaluation is crucial, we also present an algorithm to build a map that includes information over obstacle distance estimates while taking into account the level of uncertainty in each estimate. We finally show how the constructed map can be used to increase global navigation safety by planning trajectories which avoid areas of high uncertainty, enabling higher autonomy for mobile robots in indoor settings.

I. INTRODUCTION

Deep Neural Networks (DNNs) have recently found increasing adoption in robotics, where they are being proposed for applications such as grasping [1] and autonomous navigation [2]. This is, however, raising concerns over Artificial Intelligence (AI) safety [3], especially in situations where unreliable predictions can cause damage to expensive hardware or even human harm, as in the case of the recent accidents involving autonomous vehicles, where for example the failure of a car perception system in recognizing the presence and distance of an obstacle lead to a fatal crash in May 2016. In order to integrate Deep Learning (DL) into applications, it is therefore important that DL systems are able to produce reliable estimates of the uncertainty associated with their predictions.

Autonomous navigation of mobile robots is one of the areas where AI safety is of utmost importance, both in regards to autonomous cars and to robots designed to be employed in industrial settings, since the robots are often big enough to potentially damage the environment or harm the users. Autonomous cars often employ a wide array of sensors to estimate the state of their surroundings; on the other hand, most indoor mobile robots rely only on 2D laser scanners

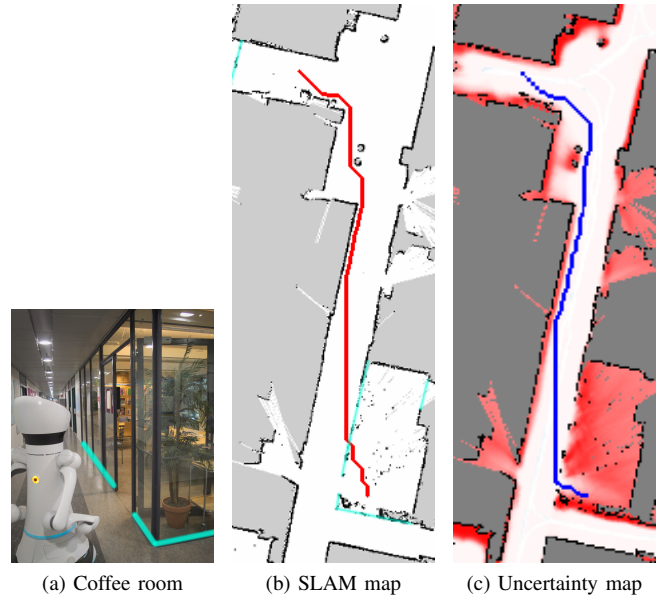


Fig. 1. Global path planning using D* on different maps. The glass surfaces are highlighted in (a) and (b) in cyan (best viewed in color).

for navigation, mapping and localization as they provide distance measurements at fast rates and in wide angular fields [4]. However, 2D laser scans offer a limited amount of information that may be insufficient for tasks like object detection and obstacle avoidance. In particular, 2D lidars are not able to detect transparent obstacles, *e.g.*, glass, and are limited to measuring occupancy at a single height, incapable of inferring the true occupancy of complex objects such as tables. For example, Figure 1b shows a trajectory planned on a map built using 2D lidars only; a robot following that path would collide with the glass walls of the coffee room shown in Figure 1a, which are invisible to the laser scanners.

To overcome these limitations, we recently proposed the use of DNNs [5], where an autoencoder was trained to infer, or *hallucinate*, the actual distance of objects from raw 2D laser input. We refer to this distance as the *robot-to-obstacle distance*, *i.e.*, “the distance along a certain direction to the closest point of an obstacle that the robot could collide with.” We demonstrated the ability of the approach to estimate the occupancy of complex objects (*i.e.*, tables and glass walls), and how the approach could improve safety for local navigation; however, the approach provides point estimates which are subject to noise. This motivated us to explore how to predict the uncertainty of these robot-to-obstacle distances and its application to indoor navigation. The most practical and widely adopted approach to predict uncertainty

*These authors contributed equally to this paper.

This work was supported by Academy of Finland, decision 314180.

J. Lundell, F. Verdoja and V. Kyrki are with School of Electrical Engineering, Aalto University, Finland. `name.surname@aalto.fi`

of deep models is known as Monte-Carlo (MC) Dropout [6]. However, it has been shown that the application of MC Dropout to some domains can be problematic [7]–[9], and we demonstrate how it cannot be used effectively for the task at hand. We then propose an alternative DL-based method which is able to produce adequate prediction of uncertainty. Also, we demonstrate how the inclusion of uncertainty can be exploited for building an uncertainty map of the environment to be used for safer global navigation. Figure 1c shows an example of such maps, where trajectories can be planned to avoid areas of high uncertainty—marked in red—resulting in safer paths.

The main contributions of this study are: (1) a novel DL-based approach for uncertainty prediction and its application in the domain of robot-to-obstacle distance estimation from raw 2D laser data; (2) an algorithm for building uncertainty maps of indoor environments that can be used to integrate uncertainty predictions in global navigation frameworks; (3) an empirical comparison of the proposed technique with the de-facto standard MC Dropout for the task at hand, showing how the proposed approach is a better choice in this domain.

The paper is structured as follows: in Section II we review relevant works in the state-of-the-art, while the proposed approach for uncertainty estimation and the pipeline for exploiting it in navigation are presented in Section III and evaluated in Section IV. In Section V conclusions are drawn and future directions are proposed.

II. RELATED WORKS

A. Uncertainty in robotic mobility

In the context of robotic mobility, we recognize three different areas where recent research addressed uncertainty: (1) localization, where the goal is to reduce uncertainty regarding the robot position in relation to a known environment; (2) local navigation, where robot movements should account for sensor uncertainty over obstacle position and occupancy; and (3) mapping and global navigation, where planned trajectories should avoid areas whose content is uncertain, and prefer paths free from obstacles where a robot can safely navigate. We will focus here on reviewing them separately, but it is worth mentioning that when considering the Simultaneous Localization and Mapping (SLAM) problem they have to be accounted for at the same time; also, in this case, even more uncertainty arises from the interplay between them [10].

a) Localization: Evaluating pose uncertainty in known environments is a widely studied problem, where several approaches have been proposed over many years of research, including Monte-Carlo sampling over the distribution of possible positions [11], the use of belief spaces and belief trees [12], [13] and a recent DL-based localization method designed to actively reduce uncertainty [14]. Although localization uncertainty has been studied for many years, it is still recognized as an open and important problem [10]. Nevertheless, it is out of scope of this paper.

b) Local navigation: Ensuring safety in the context of local navigation requires to estimate from sensory data the position and occupancy of obstacles surrounding the robot. To achieve this task robots often rely on raw 2D laser data, despite laser sensors inherent limitation in providing correct distance estimates for many complex objects, including tables, chairs, windows, and open shelves. A recent paper [15] presented a method for planning theoretically safe paths in environments sensed by a 2D lidar. The authors propose to inflate obstacles by a volume that represented both the pose uncertain and the space the obstacle might occupy. However, the experimental demonstration is limited to simple objects and no advice is given on how to address more complex objects. Another option to reduce obstacle uncertainty is sensor fusion [4], [16], but such approaches typically require visual sensors that suffer from limited field of view and higher processing time.

We recently shifted the focus from estimating obstacle occupancy from raw 2D laser data towards learning to infer robot-to-obstacle distances using neural networks [5]. The results demonstrated first of all that typical indoor environments include enough structure to learn the robot-to-obstacle distance of objects such as tables and windows, and secondly that the learned robot-to-obstacle distance can improve local navigation safety. However, that work did not address obstacle position uncertainty, but rather focused on situations where raw laser readings could not capture the actual robot-to-obstacle distance and in those cases tried to produce better estimates. In this paper, on the other hand, we address the problem of how the uncertainty of the deep model used to produce that estimate can be predicted and exploited.

c) Mapping and global navigation: Known indoor environments are often represented as occupancy grids, where each cell represents a portion of the environment that is either free, occupied or unknown. When a robot has to plan a path to a particular pose, it searches for a trajectory through the free space that reaches the goal position at a minimum cost, according to a predefined cost function. Most of the times, these maps are built through accumulation of evidence by running the robot in the environment. This process naturally lends itself to account for uncertainty, as effectively each cell contains the belief of it being occupied. However, occupancy maps are usually thresholded and used in the aforementioned ternary form [17]. Uncertainty is then accounted for in different ways, *e.g.*, through planning in a belief state over obstacle positions to minimize path uncertainty [18] or by inflating or deflating obstacles depending on collision probability [19].

A recent paper presented a method for fusing measurement uncertainty directly into the map [20]. That work, however, assumed uncertainty stemmed from noisy measurement and not from the inability to detect the occupancy of objects in the environment. In this work, on the other hand, it is defined as the uncertainty of a deep model estimating robot-to-obstacle distances. This enables building uncertainty maps that not only contain actual object occupancies but also their positional uncertainty. These uncertainty maps are an

interesting step forward from ternary occupancy maps and in this work we present a method for building such maps.

B. Deep model uncertainty

Standard DL architectures provide point estimates, but do not inherently capture model uncertainty. Uncertainty can, however, be evaluated with Bayesian Neural Networks (BNNs) [21], [22] where deterministic weights are replaced with distributions over the parameters. Although BNNs are relatively easy to formulate, using them to perform inference is impractical as it is often impossible to analytically evaluate the marginal probability required for training. Recent new variational inference methods have been proposed to address this issue, however they still come with increased computational cost, requiring often double the number of parameters to represent uncertainty [6], [23].

Another possibility to model uncertainty in DNNs that has attracted a lot of interest recently is to use dropout as approximate Bayesian variational inference [6]. The key idea is to enable dropout not only in training but also during testing, do several forward passes through the network with the same input data, and as a final step estimate the first two moments (mean and variance) of the predictive distribution. The mean is then used as estimate, and the variance as a measure of uncertainty. Using this approach, researchers have increased semantic segmentation performance on images [24] and visual relocalization accuracy [25]. Despite the success behind using this approach, known as MC Dropout, in estimating uncertainty in deep models, there are scenarios where the approach does not generate reasonable results [7]–[9]. In particular, analysis by Osband [8] indicates that the variance from MC Dropout is correlated with the predicted mean. In Section IV, we provide experimental evidence for this effect, which prevents using MC Dropout in the context of this work, where the impact of the mean on the variance estimate is strong.

III. METHOD

In this section, we describe an approach for predicting uncertainty of distance estimates and how to integrate it when building occupancy maps. Following the formalism presented in [5], let us define the output of a generic N -point 2D laser positioned at a height h from floor level as a 1D vector $\mathbf{l}_h = \{l_{ih}\}_{i=1}^N$ where each l_{ih} represents an estimate (usually, in meters) of the distance d_{ih} of closest obstacle from the laser at height h , along the direction i . When considering a specific robot with height H and a 2D laser sensor positioned at a fixed height $h^* \in [0, H]$, we define the vector $\mathbf{x} = \mathbf{l}_{h^*}$. The robot-to-obstacle distances are represented as the closest point along each direction,

$$\mathbf{y} = \{y_i \mid y_i = \min_{h \in [0, H]} d_{ih}\}_{i=1}^N. \quad (1)$$

Let $\hat{\mathbf{y}}$ be an estimate of \mathbf{y} , given from a function approximator \mathcal{H} that takes raw 2D laser signal \mathbf{x} as input. Such a function approximator was introduced in our original work [5]. In this work, we develop a method to predict the uncertainty of the estimator \mathcal{H} .

A. Uncertainty models

Assuming independence between each data point, the likelihood that $\hat{\mathbf{y}} = \mathcal{H}(\mathbf{x})$ follows a parametric model with parameter θ is

$$\mathcal{L}(\hat{\mathbf{y}} \mid \theta) = \prod_{i=1}^N p(\hat{y}_i \mid \theta). \quad (2)$$

We are interested in a model that enable us to maximize \mathcal{L} , or, more practically, the log-likelihood $\ell(\hat{\mathbf{y}} \mid \theta) = \ln \mathcal{L}(\hat{\mathbf{y}} \mid \theta)$. A common choice is to assume the uncertainty follows a Gaussian model, as in the case of MC Dropout [6], [26].

Under such assumption, one can center the distribution on the true robot-to-obstacle distance y_i and represent the uncertainty using the model standard deviation by finding an uncertainty vector $\hat{\mathbf{u}} = \{\hat{u}_i\}_{i=1}^N$ such that $\hat{\mathbf{u}} = \arg \max_{\hat{\mathbf{u}} \in \mathbb{R}_+^N} \ell_{\mathcal{N}}(\hat{\mathbf{y}} \mid \mathbf{y}, \hat{\mathbf{u}})$, where

$$\begin{aligned} \ell_{\mathcal{N}}(\hat{\mathbf{y}} \mid \mathbf{y}, \hat{\mathbf{u}}) &= \sum_{i=1}^N \ln p(\hat{y}_i \mid \mu = y_i, \sigma = \hat{u}_i) \\ &= \sum_{i=1}^N \ln \left(\frac{1}{\sqrt{2\pi\hat{u}_i^2}} \exp \left(-\frac{(\hat{y}_i - y_i)^2}{2\hat{u}_i^2} \right) \right) \\ &\propto - \sum_{i=1}^N \left[\ln \hat{u}_i^2 + \frac{(\hat{y}_i - y_i)^2}{\hat{u}_i^2} \right]. \end{aligned} \quad (3)$$

However, as we will demonstrate in Section IV such a model is unable to correctly represent the data considered in this work.

Another option is to assume the uncertainty follows a Laplace distribution, a choice that was shown to work well for estimating uncertainty in regression tasks in vision [26]. In this case the uncertainty is represented by the scale parameter b of the Laplace distribution by finding $\hat{\mathbf{u}} = \arg \max_{\hat{\mathbf{u}} \in \mathbb{R}_+^N} \ell_L(\hat{\mathbf{y}} \mid \mathbf{y}, \hat{\mathbf{u}})$, where

$$\begin{aligned} \ell_L(\hat{\mathbf{y}} \mid \mathbf{y}, \hat{\mathbf{u}}) &= \sum_{i=1}^N \ln p(\hat{y}_i \mid \mu = y_i, b = \hat{u}_i) \\ &= \sum_{i=1}^N \ln \left(\frac{1}{2\hat{u}_i} \exp \left(-\frac{|\hat{y}_i - y_i|}{\hat{u}_i} \right) \right) \\ &\propto - \sum_{i=1}^N \left[\ln \hat{u}_i + \frac{|\hat{y}_i - y_i|}{\hat{u}_i} \right]. \end{aligned} \quad (4)$$

B. Network architecture

We propose to train an autoencoder \mathcal{U} to estimate $\hat{\mathbf{u}}$. Figure 2 shows schematically the proposed architecture. The network is divided in two components. The first is an encoder φ that takes as input a 2D matrix of length $N = 128$ obtained by concatenating \mathbf{x} and $\hat{\mathbf{y}}$ over the second dimension. It then passes this 128×2 input through four 1D convolutional layers (kernel size $K = 5$, stride $S = 2$), connected via Batch Normalization (BN) [27] and Rectified Linear Unit (ReLU) [28] layers. The output sizes of the convolutional layers are, in order, 64×16 , 32×32 ,

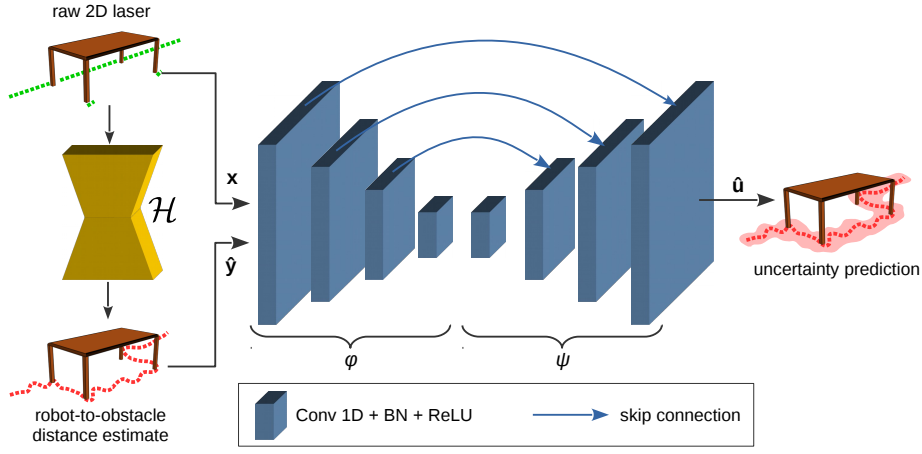


Fig. 2. The proposed fully convolutional autoencoder \mathcal{U}

16×64 , and 8×128 . The output of φ is the input to the second part of the network: the decoder ψ , which has the same structure as φ , and outputs a 1D vector $\hat{\mathbf{u}}$ of size N through a series of 1D transposed deconvolutional layers ($K = 5$, $S = 2$), also connected via BN and ReLU. The size of the layers' outputs are the opposite to the encoder's, *i.e.*, 16×64 , 32×32 , 64×16 , and 128×1 . Corresponding convolutional and deconvolutional layers are connected through skip connections, as their ability to improve the performance of the network has been demonstrated in this domain [5]. The input of the network is scaled to the range $[0, 1]$ to improve convergence speed, and weights are optimized using Adaptive Moment Estimation (Adam). Depending on which uncertainty (Gaussian or Laplacian) the network should model, the loss function it minimizes is either the negative log-likelihood of (3) or (4). It is worth noticing that although in this work we limit the study to those two models, the proposed method can work with any other parametric distribution.

C. Building an uncertainty map

Next we present a method for building occupancy maps that incorporates both the robot-to-obstacle distance prediction and its uncertainty. To create these maps—which we call *uncertainty maps*—we adapt standard occupancy mapping techniques [17] to account for our uncertainty estimates similarly to [20], [29]. In the following, we will present the construction for an uncertainty model following Laplacian distribution; however, the construction for a Gaussian model is similar and is discussed in detail in [20].

The occupancy probability $P(c = 1|\hat{y}_r)$ of a cell c given an estimated robot-to-obstacle distance \hat{y}_r along a laser ray r is defined as

$$P(c = 1|\hat{y}_r) = \int_0^\infty P(c = 1|y_r)P(y_r|\hat{y}_r)dy_r, \quad (5)$$

where y_r represents the true robot-to-obstacle distance along ray r . Here, we model the occupancy given the true robot-to-obstacle distance $P(c = 1|y_r)$ as 0 in front of the obstacle, 1

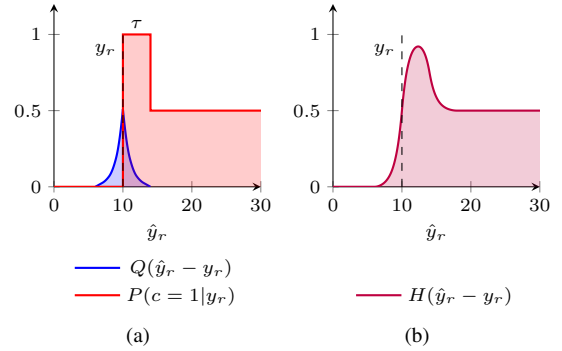


Fig. 3. The geometric construction of $P(c = 1|y_r)$, where τ equals half the support of Q (a), and the resulting convolution (b).

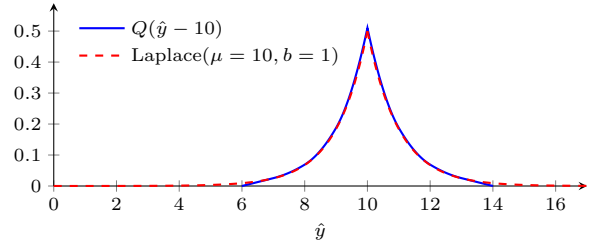


Fig. 4. The quadratic B-spline function Q , and the corresponding Laplace.

from the surface to τ units behind, and then 0.5. An example of $P(c = 1|y_r)$ is shown in red in Figure 3a.

Calculating the integral in (5) requires a model $P(y_r|\hat{y}_r)$ of the true robot-to-obstacle distance given a noisy measurement reading. As stated in Section III, $P(y_r|\hat{y}_r)$ is modeled as a Laplace distribution. However, as pointed out in [29], integrating (5) over a distribution with infinite support results in obstacles lying slightly behind the range measurement even when the measurements are precise. One solution is to set $\tau = \infty$, but this can degenerate occupancy probabilities [29]. Another, more stable, option is to limit the support of $P(y_r|\hat{y}_r)$. In this work, similarly to [29], the support of a Laplace distribution is limited by approximating it as a

Algorithm 1 Uncertainty Map

Inputs: \mathbf{P} : Robot poses, \mathbf{L} : Laser scans,
 \mathbf{M} : Empty map, α : Correlation factor.

```
for all  $p \in \mathbf{P}$  do  
   $\mathbf{x} \leftarrow \text{GETLASERSCAN}(\mathbf{L}, p)$   
   $\hat{\mathbf{y}} \leftarrow \mathcal{H}(\mathbf{x})$   
   $\hat{\mathbf{u}} \leftarrow \mathcal{U}(\mathbf{x}, \hat{\mathbf{y}})$   
  for all  $r \in 1, \dots, N$  do  
     $\mathbf{C} \leftarrow \text{RAYCAST}(p, \hat{\mathbf{y}}_r)$   
    for all ( $c \in \mathbf{C}$ ) do  
       $d_{c\hat{\mathbf{y}}_r} \leftarrow \text{EUCLIDDIST}(c, \hat{\mathbf{y}}_r)$   
       $o_c \leftarrow H\left(\frac{d_{c\hat{\mathbf{y}}_r} - \hat{\mathbf{y}}_r}{\hat{u}_r}\right)$   
       $m_c \leftarrow \log \frac{o_c}{1 - o_c}$   
       $\mathbf{M}(c) \leftarrow \mathbf{M}(c) + \alpha m_c$   
    end for  
  end for  
end for  
return  $\frac{1}{1 + \exp(\mathbf{M})}$ 
```

quadratic B-spline $Q(t) \approx P(y_r | \hat{y}_r)$ where $t = (y_r - \hat{y}_r) / \hat{u}_r$ and $\hat{u}_r = \mathcal{U}(x_r, \hat{y}_r)$. We derived Q numerically by imposing it to have finite support $[-4, 4]$ and unit integral. The choice of the range for the support comes down from the fact that, for a $\text{Laplace}(0, 1)$, around 99% of the cumulative distribution lies in that range. Figure 4 shows the resulting spline approximation.

By choosing the thickness term $\tau = 4\hat{u}_r$, *i.e.*, half the support of the approximated B-spline, (5) has the following analytical solution

$$P(c = 1 | \hat{y}_r) \approx H(t) = Q_{\text{cdf}}(t) - \frac{1}{2}Q_{\text{cdf}}(t - 4), \quad (6)$$

where $Q_{\text{cdf}}(t)$ is the cumulative density function of the quadratic B-spline $Q(t)$. The per-ray occupancy probability is visualized in Figure 3b.

The method for creating uncertainty maps with occupancy probabilities calculated in (6) is summarized in Algorithm 1. We assume robot poses \mathbf{P} and original laser scans \mathbf{L} to be given. First for each robot pose p , the algorithm extracts the associated original laser scan \mathbf{x} . This laser scan is then propagated through network \mathcal{H} to estimate the robot-to-obstacle distance $\hat{\mathbf{y}}$ which, together with the original laser, is propagated through \mathcal{U} to estimate the scale parameters $\hat{\mathbf{u}}$ of the Laplacian uncertainty model. Next, the algorithm goes through every laser ray $\hat{\mathbf{y}}_r$ in the current scan $\hat{\mathbf{y}}$ and finds all cells \mathbf{C} that are touched by the laser ray r originating from the current pose p . Then the algorithm iterates over each cell $c \in \mathbf{C}$, calculates the distance $d_{c\hat{\mathbf{y}}_r}$ between the center of the cell and the estimated obstacle distance $\hat{\mathbf{y}}_r$, calculates the occupancy for that cell using (6) with $t = (d_{c\hat{\mathbf{y}}_r} - \hat{\mathbf{y}}_r) / \hat{u}_r$, converts the occupancy to *log-odds*, scales it with a correlation factor α , and finally adds it to the previous occupancy value for that cell. As a final step the uncertainty map \mathbf{M} is converted from *log-odds* to occupancy probability, *i.e.*, in $[0, 1]$.

TABLE I

LOG-LIKELIHOOD OVER THE TEST SET

Algorithm	Model	$\ell(\hat{\mathbf{y}} \mathbf{y}, \hat{\mathbf{u}})$
MC Dropout	Gaussian	-2017006.82
Ours	Gaussian	-1086886.69
Ours	Laplace	2.24

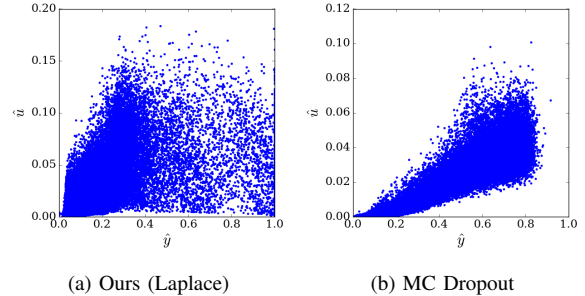


Fig. 5. Plots of the relationship between the estimated robot-to-obstacle distance $\hat{\mathbf{y}}$ and uncertainty $\hat{\mathbf{u}}$ for the proposed method and MC Dropout.

The correlation factor $0 < \alpha < 1$ limits the effect for which highly correlated readings could produce overconfident maps and remove most of the uncertainty. This parameter should be set as a function of the amount of correlation between successive readings; in this work we experimentally set it to a constant value $\alpha = 0.01$ as we are working in a static environment. In a dynamic environment, α can be set as a function of the time passed between readings to have the map adapt to changes in the environment [20].

IV. EXPERIMENTS

A. Dataset and network training

We used the same setup as in [5] to train the network \mathcal{H} . Then, to train the uncertainty network \mathcal{U} , we took the complete training and test set, propagated each laser scan \mathbf{x} through the trained network \mathcal{H} , saved each pair $(\mathbf{x}, \hat{\mathbf{y}})$ as training input, and kept \mathbf{y} to be used as ground-truth to compute the loss as explained in Section III-B. We saved these new input-output pairs as a new dataset. This dataset was then randomly split into 80% training and 20% test set and used for training the network \mathcal{U} . The reason for merging the two datasets is that the errors produced by \mathcal{H} over the training set differs slightly compared to the test set, due to the training process; thus, randomly splitting the merged dataset to train \mathcal{U} limits overfitting. The resulting training and test datasets consist of 31606 and 7902 samples respectively. The network was trained for 2000 epochs, with a batch size of 32, and learning rate set to 10^{-4} .

B. Model quality evaluation

To evaluate the quality of the proposed uncertainty model we compare its performance to that obtained by state-of-the-art MC Dropout [6]. To obtain MC Dropout’s results we modified the network in [5] to include dropout layers after each convolutional layer. We will refer to this modified

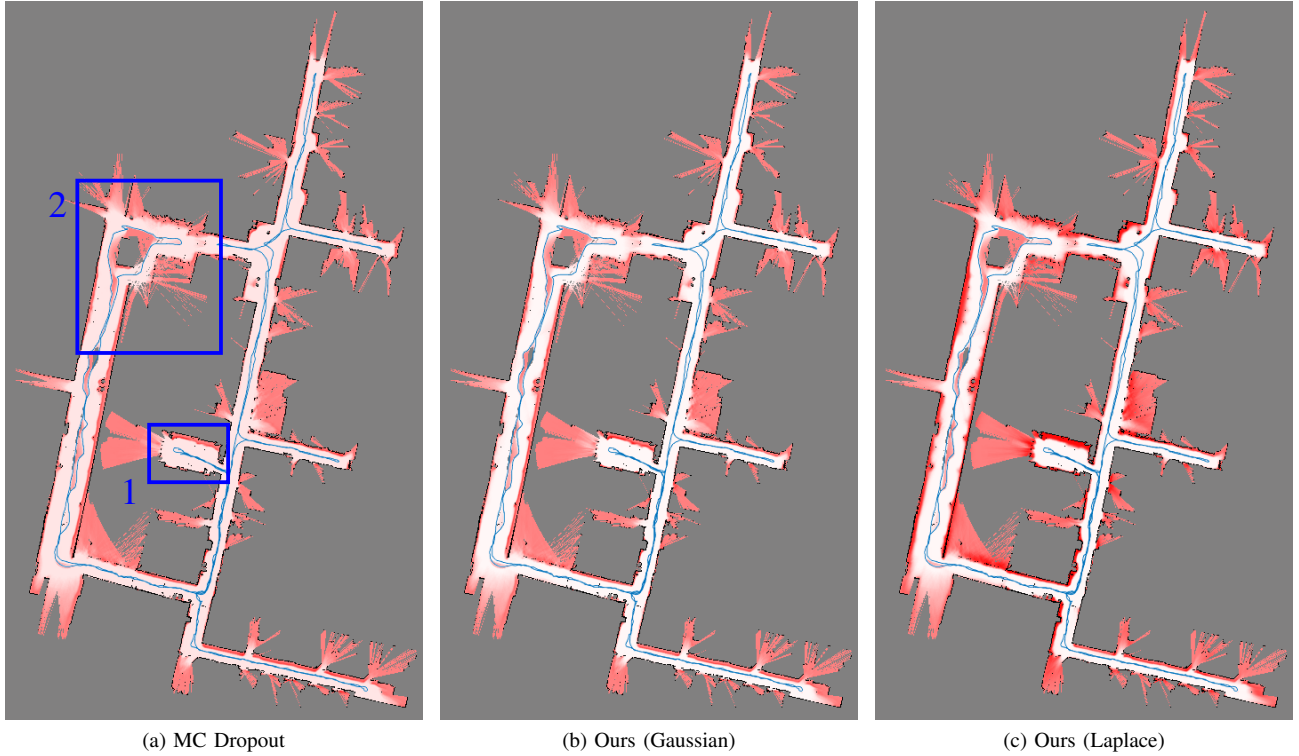


Fig. 6. The maps created by gathering data with a Care-O-bot 4. In all figures the original SLAM map is visualized in gray scale while the superimposed uncertainty maps shown in degrees of red. As in regular occupancy maps, darker red indicates a higher occupancy probability. The blue line is the robot path (best viewed in color).

version of \mathcal{H} as \mathcal{H}_D . We then trained the network with a dropout rate of 50%. In testing, to evaluate uncertainty, we performed 50 forward passes of the same input in the network using the same dropout rate. We then took the average of this sampling process as the network prediction for the robot-to-obstacle distance \hat{y} and the variance of the samples as the estimated uncertainty \hat{u} , as proposed in [6].

Table I shows log-likelihood scores for our approach, both using Gaussian and Laplacian models, compared to MC Dropout. It can be noticed how both methods using Gaussian model are unable to correctly model uncertainty of robot-to-obstacle distances and get considerably lower scores than our approach using Laplacian distribution. This makes impossible to use an approach like MC Dropout for the application at hand; given that it assumes by design the uncertainty to be Gaussian. Our approach instead, given its ability to be optimized with any distribution, is able to be used effectively, *e.g.*, by selecting a Laplacian model.

Moreover, Figure 5 presents plots comparing our approach to MC Dropout. Each plot represents results over the whole test set where each point corresponds to one lidar distance reading. It can be noticed how in Figure 5b there is a strong correlation between \hat{u} and \hat{y} . No similar effect is present in Figure 5a. This side-effect of MC Dropout, which was theoretically noted in [8], is therefore confirmed by our empirical evaluation, demonstrating that the use of MC Dropout may not be suitable for domains, like the one at hand, where there is a wide range of possible output values.

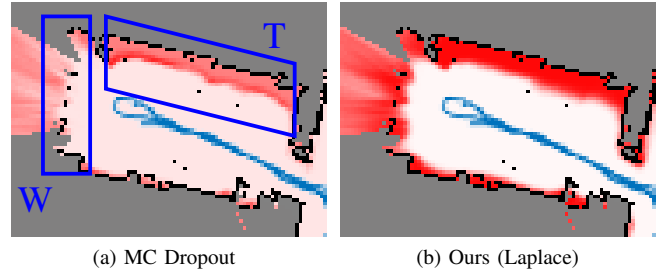


Fig. 7. Magnified area corresponding to the one marked as (1) in Figure 6a (best viewed in color).

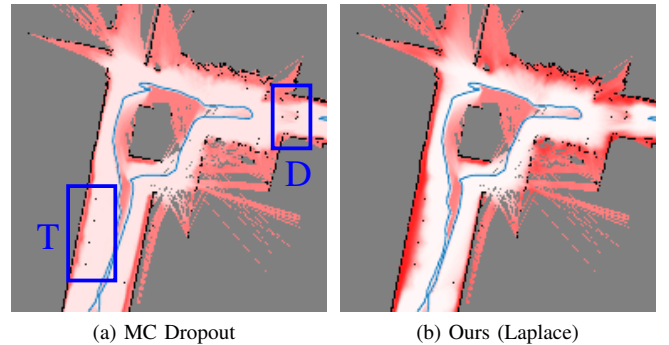


Fig. 8. Magnified area corresponding to the one marked as (2) in Figure 6a (best viewed in color).

C. Uncertainty maps

Building an uncertainty map requires robot poses, laser scans, and the inverse measurement model. To achieve this we first teleoperated a Care-O-bot 4 in our facility to gather odometry and laser range data, then we built the SLAM map shown in Figure 6 using ROS gmapping, and finally we ran ROS amcl¹ to register robot poses depicted as the blue path in Figure 6.

Once laser measurements and odometry were collected, we created, in addition to the base SLAM map, three other maps: a map obtained using MC Dropout (Figure 6a), and two different maps using our proposed approach, one modeling the uncertainty as a Gaussian distribution (Figure 6b) and another one modeling it as a Laplace (Figure 6c). All three maps were created using Algorithm 1 with $\alpha = 0.01$, where the only difference were in determining \hat{u} which for the maps in Figures 6c and 6b was set as the output from the uncertainty net, while for the MC Dropout map in Figure 6a was set as the standard deviation of the output obtained from 50 forwards passes of the same input through the network \mathcal{H}_D .

Magnified sections of these maps are shown in Figures 7 and 8. From visually inspecting these figures one can conclude that the uncertainty maps (visualized as the red shaded area) are coherent with the original SLAM map in areas with low uncertainty such as for walls, while differing in less certain areas such as for windows (W), tables (T), and glass doors (D), marked in the figures with the respective letters. Additionally, our Gaussian uncertainty map and the MC Dropout map are very similar, where the main difference is that the MC Dropout map is more uncertain about cells that are clearly free including the robot path.

With regards to the map in Figure 6a produced by MC Dropout, it is worth noticing that although the map looks reasonable thanks to the good estimate of the distance, the estimate of the uncertainty in that map is inaccurate, as demonstrated in Section IV-B. This causes the map to underestimate the occupancy of obstacles: given the correlation between the uncertainty and the estimated distance (see Figure 5b): when the robot is very close, any estimate is taken as certain. This is apparent in particular in Figures 7 and 8, where the MC Dropout map cannot capture the occupancy of T, D, and W, which our Laplace map estimates correctly.

V. CONCLUSIONS

We presented a method for predicting model uncertainty of a deep network estimating robot-to-obstacle distance and we proposed a mapping algorithm to create uncertainty maps for indoor autonomous global navigation. To achieve this we trained an uncertainty network shaped as an autoencoder that takes both estimated and original laser readings as inputs and outputs an uncertainty measure over the estimated distances. In the quantitative evaluation when the uncertainty network modeled uncertainties as Laplacian opposed to Gaussian

it produced much better predictions in comparison to the state-of-the-art MC Dropout, indicating that wider tailed distributions are better equipped to capture uncertainties in this domain. Extension of this idea to other domains is left as future work.

The ability of the Laplacian model to better represent obstacle distances is also apparent when creating uncertainty maps, where the map built using our Laplacian strategy successfully marked otherwise invisible objects such as glass as occupied, while the map build using Gaussian model did not capture such areas due to the overconfident uncertainty estimates. In addition, we demonstrated that paths planned on an uncertainty map prefer areas of lower uncertainty, increasing autonomous navigation safety over the use of traditional ternary occupancy maps.

Finally it is worth mentioning that although the proposed architecture was only tested in this domain, it is agnostic to the shape of the estimator \mathcal{H} and to the data it is processing, indicating that it may generalize to model uncertainties in other domains as well. However, generalization of this architecture is out of the scope of this study and is left as future work.

REFERENCES

- [1] J. Varley, C. DeChant, A. Richardson, J. Ruales, and P. Allen, "Shape completion enabled robotic grasping," in *2017 IEEE/RSJ International Conference on Intelligent Robots and Systems (IROS)*, Sept. 2017, pp. 2442–2447.
- [2] M. Pfeiffer, M. Schaeuble, J. Nieto, R. Siegwart, and C. Cadena, "From perception to decision: A data-driven approach to end-to-end motion planning for autonomous ground robots," in *Robotics and Automation (ICRA), 2017 IEEE International Conference on*. IEEE, 2017, pp. 1527–1533.
- [3] D. Amodei, C. Olah, J. Steinhardt, P. Christiano, J. Schulman, and D. Mané, "Concrete Problems in AI Safety," *arXiv:1606.06565 [cs]*, June 2016. [Online]. Available: <http://arxiv.org/abs/1606.06565>
- [4] H. Baltzakis, A. Argyros, and P. Trahanias, "Fusion of laser and visual data for robot motion planning and collision avoidance," *Machine Vision and Applications*, vol. 15, no. 2, pp. 92–100, Dec. 2003.
- [5] J. Lundell, F. Verdoja, and V. Kyrki, "Hallucinating robots: Inferring obstacle distances from partial laser measurements," *arXiv:1805.12338 [cs, eess, stat]*, 2018. [Online]. Available: <http://arxiv.org/abs/1805.12338>
- [6] Y. Gal and Z. Ghahramani, "Dropout As a Bayesian Approximation: Representing Model Uncertainty in Deep Learning," in *Proceedings of the 33rd International Conference on International Conference on Machine Learning*, ser. ICML'16, vol. 48, New York, NY, USA, 2016, pp. 1050–1059.
- [7] I. Osband, C. Blundell, A. Pritzel, and B. Van Roy, "Deep Exploration via Bootstrapped DQN," in *Advances in Neural Information Processing Systems 29 (NIPS 2016)*, D. D. Lee, M. Sugiyama, U. V. Luxburg, I. Guyon, and R. Garnett, Eds. Curran Associates, Inc., 2016, pp. 4026–4034.
- [8] I. Osband, "Risk versus Uncertainty in Deep Learning: Bayes, Bootstrap and the Dangers of Dropout," in *NIPS 2016 Workshop on Bayesian Deep Learning*, Barcelona, Spain, Dec. 2016.
- [9] T. Pearce, N. Anastassacos, M. Zaki, and A. Neely, "Bayesian Inference with Anchored Ensembles of Neural Networks, and Application to Reinforcement Learning," *arXiv:1805.11324 [cs, stat]*, May 2018. [Online]. Available: <http://arxiv.org/abs/1805.11324>
- [10] M. L. Rodríguez-Arévalo, J. Neira, and J. A. Castellanos, "On the Importance of Uncertainty Representation in Active SLAM," *IEEE Transactions on Robotics*, vol. 34, no. 3, pp. 829–834, June 2018.
- [11] F. Dellaert, D. Fox, W. Burgard, and S. Thrun, "Monte Carlo localization for mobile robots," in *Proceedings 1999 IEEE International Conference on Robotics and Automation (Cat. No.99CH36288C)*, vol. 2, 1999, pp. 1322–1328.

¹gmapping: <http://wiki.ros.org/gmapping> – amcl: <http://wiki.ros.org/amcl>

- [12] S. Prentice and N. Roy, "The Belief Roadmap: Efficient Planning in Belief Space by Factoring the Covariance," *The International Journal of Robotics Research*, vol. 28, no. 11-12, pp. 1448–1465, Nov. 2009.
- [13] A. Bry and N. Roy, "Rapidly-exploring Random Belief Trees for motion planning under uncertainty," in *2011 IEEE International Conference on Robotics and Automation*, May 2011, pp. 723–730.
- [14] D. S. Chaplot, E. Parisotto, and R. Salakhutdinov, "Active Neural Localization," *arXiv:1801.08214 [cs]*, Jan. 2018. [Online]. Available: <http://arxiv.org/abs/1801.08214>
- [15] B. Axelrod, L. Kaelbling, and T. Lozano-Perez, "Provably Safe Robot Navigation with Obstacle Uncertainty," in *Proceedings of Robotics: Science and Systems XIII*, Cambridge, Massachusetts, USA, July 2017.
- [16] Y. Liao, L. Huang, Y. Wang, S. Kodagoda, Y. Yu, and Y. Liu, "Parse geometry from a line: Monocular depth estimation with partial laser observation," in *2017 IEEE International Conference on Robotics and Automation (ICRA)*, May 2017, pp. 5059–5066.
- [17] S. Thrun, W. Burgard, and D. Fox, *Probabilistic Robotics (Intelligent Robotics and Autonomous Agents)*. The MIT Press, 2005.
- [18] R. Valencia, J. Andrade-Cetto, and J. M. Porta, "Path planning in belief space with pose SLAM," in *2011 IEEE International Conference on Robotics and Automation*, May 2011, pp. 78–83.
- [19] L. Janson, E. Schmerling, and M. Pavone, "Monte Carlo Motion Planning for Robot Trajectory Optimization Under Uncertainty," in *Robotics Research*, A. Bicchi and W. Burgard, Eds. Cham: Springer International Publishing, 2018, vol. 3, pp. 343–361.
- [20] E. Vespa, N. Nikolov, M. Grimm, L. Nardi, P. H. J. Kelly, and S. Leutenegger, "Efficient Octree-Based Volumetric SLAM Supporting Signed-Distance and Occupancy Mapping," *IEEE Robotics and Automation Letters*, vol. 3, no. 2, pp. 1144–1151, 2018.
- [21] J. S. Denker and Y. Lecun, "Transforming neural-net output levels to probability distributions," in *Advances in neural information processing systems*, 1991, pp. 853–859.
- [22] D. J. C. MacKay, "A Practical Bayesian Framework for Backpropagation Networks," *Neural Computation*, vol. 4, no. 3, pp. 448–472, May 1992.
- [23] C. Blundell, J. Cornebise, K. Kavukcuoglu, and D. Wierstra, "Weight Uncertainty in Neural Network," in *International Conference on Machine Learning*, June 2015, pp. 1613–1622.
- [24] A. Kendall, V. Badrinarayanan, and R. Cipolla, "Bayesian SegNet: Model Uncertainty in Deep Convolutional Encoder-Decoder Architectures for Scene Understanding," *arXiv:1511.02680 [cs]*, Nov. 2015. [Online]. Available: <http://arxiv.org/abs/1511.02680>
- [25] A. Kendall and R. Cipolla, "Modelling uncertainty in deep learning for camera relocalization," in *2016 IEEE International Conference on Robotics and Automation (ICRA)*, May 2016, pp. 4762–4769.
- [26] A. Kendall and Y. Gal, "What Uncertainties Do We Need in Bayesian Deep Learning for Computer Vision?" in *Advances in Neural Information Processing Systems 30*, I. Guyon, U. V. Luxburg, S. Bengio, H. Wallach, R. Fergus, S. Vishwanathan, and R. Garnett, Eds. Curran Associates, Inc., 2017, pp. 5574–5584.
- [27] S. Ioffe and C. Szegedy, "Batch Normalization: Accelerating Deep Network Training by Reducing Internal Covariate Shift," in *PMLR*, June 2015, pp. 448–456.
- [28] K. He, X. Zhang, S. Ren, and J. Sun, "Delving Deep into Rectifiers: Surpassing Human-Level Performance on ImageNet Classification," in *2015 IEEE International Conference on Computer Vision (ICCV)*, Dec. 2015, pp. 1026–1034.
- [29] C. Loop, Q. Cai, S. Orts-Escolano, and P. A. Chou, "A Closed-Form Bayesian Fusion Equation Using Occupancy Probabilities," in *2016 Fourth International Conference on 3D Vision (3DV)*, 2016, pp. 380–388.